

Kinetics Study of the OH + Alkene → H₂O + Alkenyl Reaction ClassLam K. Huynh,[†] Kyle Barriger,[‡] and Angela Violi^{*,†,‡}

Departments of Mechanical Engineering and of Chemical Engineering, The University of Michigan, Ann Arbor, Michigan 48109-2125

Received: September 1, 2007; In Final Form: October 21, 2007

In this paper we report on the kinetics of hydrogen abstraction for the OH + alkene reaction class, using the reaction class transition state theory (RC-TST) combined with the linear energy relationship (LER) and the barrier height grouping (BHG) approaches. Parameters for the RC-TST were derived from theoretical calculations using a set of 15 reactions representing the hydrogen abstractions from the terminal and nonterminal carbon sites of the double bond of alkene compounds. Both the RC-TST/LER, where only reaction energy is needed at either density functional theory BH&HLYP or semiempirical AM1 levels, and RC-TST/BHG, where no additional information is required, are found to be promising methods for predicting rate constants for a large number of reactions in this reaction class. Detailed error analyses show that, when compared to explicit theoretical calculations, the averaged systematic errors in the calculated rate constants using both the RC-TST/LER and RC-TST/BHG methods are less than 25% in the temperature range 300–3000 K. The estimated rate constants using these approaches are in good agreement with available data in the literature.

1. Introduction

The hydrogen abstraction reaction between a hydroxyl radical (OH) and an alkene (C=C) to form a water molecule (H₂O) and an alkenyl radical (C=C•) is known to be an important reaction class in combustion processes of hydrocarbon fuel, especially in the high-temperature regime.¹ The hydrogen abstraction reaction between C₂H₄ and OH to form C₂H₃ and H₂O has attracted a number of extensive experimental as well as theoretical investigations. There are more than 15 entries for rate constant studies for this reaction in the NIST chemical kinetics database.² For reactions involving alkenes larger than C₂H₄, even fewer data are available due to the involvement of other kinds of reactions such as the addition of OH to the double bond and the hydrogen abstraction at different carbon sites, e.g., saturated carbon sites (sp³ hybridization). For example, there are only two records for rate constants for the reaction with propene (C₃H₆), either at the terminal or at the nonterminal carbon sites of the double bond.^{3,4} Both of these records were obtained indirectly using the results of similar reactions. Using the transition state theory (TST) model, Tsang³ examined the rate data reported by Tully et al.⁵ for the OH + C₂H₄ hydrogen abstraction reaction to estimate rate constants for the OH + C₃H₆ reaction at both the terminal and nonterminal carbon sites in the temperature range 700–2500 K. Alternatively, Baldwin et al.⁴ derived the rate constants for the abstraction at the terminal carbon site by fitting a complex kinetic model to experimental data for the oxidation of propene.

OH + alkene reactions are an important part of the kinetic mechanisms available in the literature to study combustion systems. It is, however, impracticable to obtain the correct kinetic data for such a large number of reactions by experiments or explicit rate-constant calculations even using the simple TST method. Alternatively, recent developments and applications of

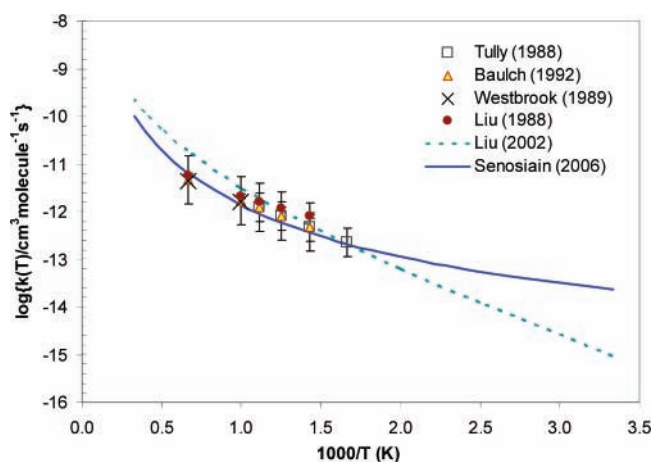


Figure 1. Arrhenius plots of the available rate constants for the OH + C₂H₄ → H₂O + C₂H₃. The error bars for these rate constants are also included.

the existing first-principles-based methods^{6,7} indicated that it is possible to predict rate constants of any reaction in this class on the fly. The practicality of using the reaction class transition state theory (RC-TST) for estimating rate constants of a large number of reactions in a given class has been shown successfully in several previous studies.^{8–13}

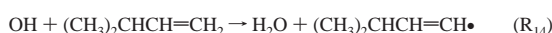
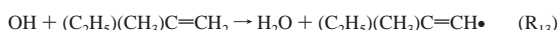
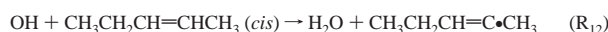
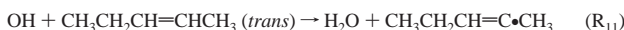
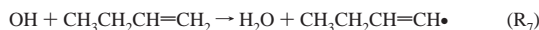
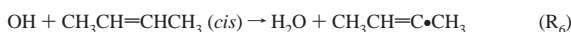
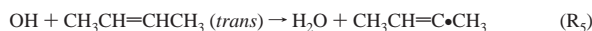
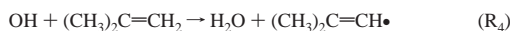
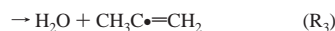
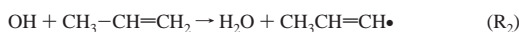
In this study, we employ the RC-TST to derive all parameters for estimating rate constants of reactions belonging to the OH + alkene class. To do so, our main task is to find correlation expressions between rate constants of the reference reaction and those of other reactions in the class from explicit direct *ab initio* dynamics calculations of the rate constants of a representative set in the class itself. The assumption is that these correlation expressions are applicable to all reactions in the class.

To compute the RC-TST parameters for the OH + alkene class, 15 reactions are considered as a representative set. These reactions are

* Corresponding author. E-mail: avioli@umich.edu.

[†] Department of Mechanical Engineering.

[‡] Department of Chemical Engineering.



where *trans* and *cis* denote *trans* and *cis* configurations for the carbon chain. Note that this set does not include reactions with resonance systems, e.g., 1,3-butadiene, as well as aromatic systems, e.g., benzene. The reason for this is given in the discussion section below.

2. Methodology

2.1. Reaction Class Transition State Theory. Because the details of the RC-TST method have been reported elsewhere,^{6,11,14,15} below we present only the main features of the approach. The basic idea of the RC-TST technique is that reactions belonging to a specific class have the same reactive moiety; thus the difference between the rate constants of any two reactions in the class is mainly due to the difference in the interactions between the reactive moiety and their different substituents. Within the RC-TST framework, the rate constants of an arbitrary reaction (denoted as k_a) are proportional to those of a reference reaction, k_r , (usually the smallest reaction in the class, which is referred to as the principal reaction) in the same class by a temperature-dependent function $f(T)$:

$$k_a(T) = f(T) k_r(T) \quad (1)$$

The rate constants for the reference reaction are often known experimentally or can be calculated accurately from first-principles. The key idea of the RC-TST method is to factor $f(T)$ into different components under the TST framework:

$$f(T) = f_\sigma f_\kappa f_Q f_V \quad (2)$$

where f_σ , f_κ , f_Q , and f_V are the symmetry number, tunneling, partition function, and potential energy factors, respectively. These terms are simply the ratios of the corresponding components in the TST expression for the arbitrary and reference reactions:

$$f_\sigma = \frac{\sigma_a}{\sigma_r} \quad (3)$$

$$f_\kappa(T) = \frac{\kappa_a(T)}{\kappa_r(T)} \quad (4)$$

$$f_Q(T) = \frac{\left(\frac{Q_a^\ddagger(T)}{\Phi_a^R(T)}\right)}{\left(\frac{Q_r^\ddagger(T)}{\Phi_r^R(T)}\right)} = \frac{\left(\frac{Q_a^\ddagger(T)}{Q_r^\ddagger(T)}\right)}{\left(\frac{\Phi_a^R(T)}{\Phi_r^R(T)}\right)} \quad (5)$$

$$f_V(T) = \exp\left[-\frac{(\Delta V_a^\ddagger - \Delta V_r^\ddagger)}{k_B T}\right] = \exp\left[-\frac{\Delta \Delta V^\ddagger}{k_B T}\right] \quad (6)$$

where σ is the reaction symmetry number, $\kappa(T)$ is the transmission coefficient accounting for the quantum mechanical tunneling effects, Q^\ddagger and Φ^R are the total partition functions (per unit volume) of the transition state and reactants, ΔV^\ddagger is the classical reaction barrier height, T is the temperature in Kelvin, and k_B is the Boltzmann constant. The potential energy factor can be calculated using the reaction barrier heights of the arbitrary reaction and the reference reaction. The classical reaction barrier height ΔV^\ddagger for the arbitrary reaction can be obtained using the linear energy relationship (LER), similar to the well-known Evans–Polanyi linear free energy relationship,^{16–18} between classical barrier heights and reaction energies in a given class without having to calculate them explicitly. Alternatively, the barrier height for the arbitrary reaction can be obtained from the barrier height group (BHG) approach where reactions in a subclass can be reasonably assumed to have the same barrier height.

In the next sections, we first determine the explicit expressions for f_σ , f_κ , f_Q , and f_V correlating the rate constants of the reference reaction (R_r) with those of the arbitrary reaction (R_a) in the same class using the representative set of reactions R_1 – R_{15} reported in the previous section and we then discuss the results using three error analyses. Once these expressions are determined, the thermal rate constant of any reaction in the OH + alkene class can be predicted from either the LER approach using the reaction energy or the BHG method with no additional information.

2.2. Computational Details. All the electronic structure calculations were carried out using the GAUSSIAN 03 program.¹⁹ Hybrid nonlocal density functional theory (DFT), particularly Becke’s half-and-half²⁰ (BH&H) nonlocal exchange and the Lee–Yang–Parr²¹ (LYP) nonlocal correlation functionals, has been found to be sufficiently accurate for predicting the transition state properties, e.g., barrier height and vibrational frequency, for hydrogen abstraction reactions by a radical.^{22–25} Note that within the RC-TST framework, as discussed above, only the relative barrier heights are needed. Our previous studies have shown that the BH&HLYP method can be employed to accurately predict relative barrier heights.^{6,15,26,27,42} Geometries of reactants, transition states, and products were optimized at BH&HLYP level of theory with the Dunning’s correlation-consistent polarized valence triple- ζ basis set denoted as cc-pVTZ,²⁸ which is sufficient to capture the physical change along the reaction coordinate for this type of reaction. Frequencies of the stationary points were also calculated at the same level of theory. This information was used to derive the RC-TST factors. The AM1 semiempirical method²⁹ was also employed to calculate the reaction energies of the reactions considered in this study. AM1 and BH&HLYP/cc-pVTZ reaction energies were then used to derive the LER’s between the barrier heights and reaction energies. Note that AM1 reaction energy is only used to extract accurate barrier heights from the LER’s, it is not directly involved in any rate calculations.

To derive the RC-TST correlation functions, TST/Eckart rate constants for all reactions in the above representative reaction

set were calculated employing the kinetic module of the web-based Computational Science and Engineering Online (CSE-Online) environment.³⁰ Thermal rate constants were computed for the temperature range 300–3000 K. Overall rotations of the species were treated classically and vibrations were treated quantum mechanically within the harmonic approximation except for the modes corresponding to the internal rotations of the CH₃ and OH groups, which were treated as the hindered rotations using the method suggested by Ayala et al.³¹ This formalism optimizes the accuracy for treating a single rotor to minimize the compound errors in the case of multiple internal rotors. To calculate the hindered rotation correction factor to the partition function for a certain vibrational mode, the rotating group and the periodicity number of the torsional potential of the vibrational mode must be identified. From the given information together with the geometry of the interested molecule, information needed for calculating the correction factor of hindered rotation treatment, e.g., reduced moment of inertia and the periodic potential, can be obtained. The correction factor is then calculated using the fitting formula (eq 26 in ref 31) derived from the tabulated accurate values to improve upon Pitzer and Gwinn's formula.^{32,33} The fitting formula keeps the good characteristics of the Pitzer and Gwinn's formula for high V_0/kT while improving its behavior for low V_0/kT , where V_0 is the internal rotation barrier height.

Previous study by Kungwan and Truong on the CH₃ + alkane reaction class¹³ has shown that the contribution of hindered rotations from alkyl groups larger than CH₃ is relatively small due to the cancellation of the treatment within the RC-TST framework (see Figure 1 in ref 11). For this reason, in this study we only consider hindered rotation treatment for the CH₃ groups.

3. Results and Discussion

In the section below, we first report on the rate constants for the reference reaction and then we describe how the RC-TST factors are derived using the training reaction set. Subsequently, we perform three error analyses to provide some estimates of the accuracy of the RC-TST method applied to this reaction class. The first error analysis is the direct comparison between the calculated rate constants and those available in the literature for reactions R₂ and R₃. The second error analysis is the comparison between the rate constants for reaction R₂–R₁₅ calculated using the RC-TST method and those obtained using the explicit full TST/Eckart method. The final analysis is on the systematic errors caused by introducing approximations in the RC-TST correlation functions.

3.1. Rate Constants of the Reference Reaction, OH + C₂H₄ → H₂O + C₂H₃. The principal reaction, OH + C₂H₄ → H₂O + C₂H₃, is chosen as the reference reaction for the OH + alkene class. Figure 1 reports the rate constants available in the literature for this reaction obtained by experiments and simulations. Tully et al.⁵ used the laser photolysis/laser-induced fluorescence technique under slow-flow conditions to measure the rate constants in the temperature range 650–901 K. Baulch et al.³⁴ presented critically evaluated kinetic data for use in computer combustion modeling. The suggested rate data with an uncertainty factor of 3 in the temperature range 650–1500 K follow closely the studies of Tully et al.⁵ Westbrook et al.³⁵ suggested rate constant data for the reference reaction in the temperature range 1003–1253 K. Using visible–UV absorption technique together with TST model, Liu et al.³⁶ reported the rates of the hydrogen abstraction in the temperature range 723–1170 K. With the energetic data obtained at the QCISD(T)/6-311G-(2df,p)/B3LYP/6-31G(d,p) together with the gradient and

Hessian information at the B3LYP/6-31G(d,p), Liu et al.³⁷ reported thermal rate constants in the temperature range 200–5000 K using the canonical variational transition state theory (CVT) and the small-curvature tunneling correction (SCT). Recently, Senosiain et al.³⁸ also carried out an analysis of the OH + C₂H₄ → H₂O + C₂H₃ reaction using the CVT method with the molecular-property data obtained at the RQCISD(T)/cc-pV ∞ Z//UB3LYP/6-311++G(d,p) level of theory to suggest rate constants for this reaction. The two rate constants obtained with the CVT theory are similar (within a deviation factor of 4) in the high-temperature regime, but they differ by an order of magnitude at lower temperature (<500 K). Because at high temperatures, the values reported by Senosiain et al. are in better agreement with the experimental data than those obtained by Liu et al. (see Figure 1), in this study we use Senosiain's expression for the rate constants of the reference reaction:

$$k_r(T) = 2.18 \times 10^{-25} T^{4.20} \exp\left[\frac{433}{T}\right] [\text{cm}^3 \text{ molecule}^{-1} \text{ s}^{-1}] \quad (7)$$

3.2. Reaction Class Parameters. *3.2.1. Potential Energy Factor.* The potential energy factor can be calculated using eq 6, where ΔV_a^\ddagger and ΔV_r^\ddagger are the barrier heights of the arbitrary and reference reactions, respectively. We have also shown that within a given class there is a linear energy relationship (LER) between the barrier height and the reaction energy, similar to the well-known Evans–Polanyi linear free energy relationship.^{16–18} Thus, accurate barrier heights can be predicted from only the reaction energies. The barrier heights for reactions R₁–R₁₅ can also be grouped into two classes: terminal carbon sites of the double bond (class 1) and nonterminal carbon sites (class 2). This can be referred to as the barrier height grouping (BHG).³⁹ The observed LERs plotted against the reaction energies calculated at BH&HLYP/cc-pVTZ and AM1 levels are shown in Figure 2a,b, respectively. The substitute of an alkyl group will stabilize the radical products, thus lowering the barrier heights. For this reason the reactions at the nonterminal carbon of the double bond (class 2) have barrier heights of about 2.0 kcal/mol lower than those at the terminal sites.

The reaction energies and barrier heights for the representative reactions R₁–R₁₅ are given in Table 1. Because reaction R₁ has no alkyl substitute group, it was excluded in the construction of the LER fitting expressions. These linear fits were obtained using the least-squares fitting method and have the following expressions:

$$\Delta V^\ddagger = 0.4892\Delta E^{\text{BH\&HLYP}} + 10.772 \text{ (kcal/mol)} \quad (8a)$$

$$\Delta V^\ddagger = 0.4238\Delta E^{\text{AM1}} + 16.572 \text{ (kcal/mol)} \quad (8b)$$

The unsigned deviations of reaction barrier heights between the LERs and the direct DFT BH&HLYP/cc-pVTZ calculations generally are smaller than 0.4 kcal/mol (see Table 1). The mean unsigned deviation (MUD) of reaction barrier heights predicted from BH&HLYP and AM1 reaction energies are 0.24 and 0.29 kcal/mol, respectively. These deviations are in fact smaller than the systematic errors of the computed reaction barriers obtained from full electronic structure calculations (~1 kcal/mol). Within the RC-TST framework, only barrier height relative to that of the reference reaction is needed and in this study the energy for the reaction R₁ was found to be 11.07 kcal/mol at the BH&HLYP/cc-pVTZ level of theory (see Table 1).

Reactions with resonance systems, e.g., 1,3-butadiene, as well as aromatic systems, e.g., benzene, are not included in this study. It is expected that the aromatic system behaves differently.³⁹ In particular, for the nonaromatic resonance systems, it is found

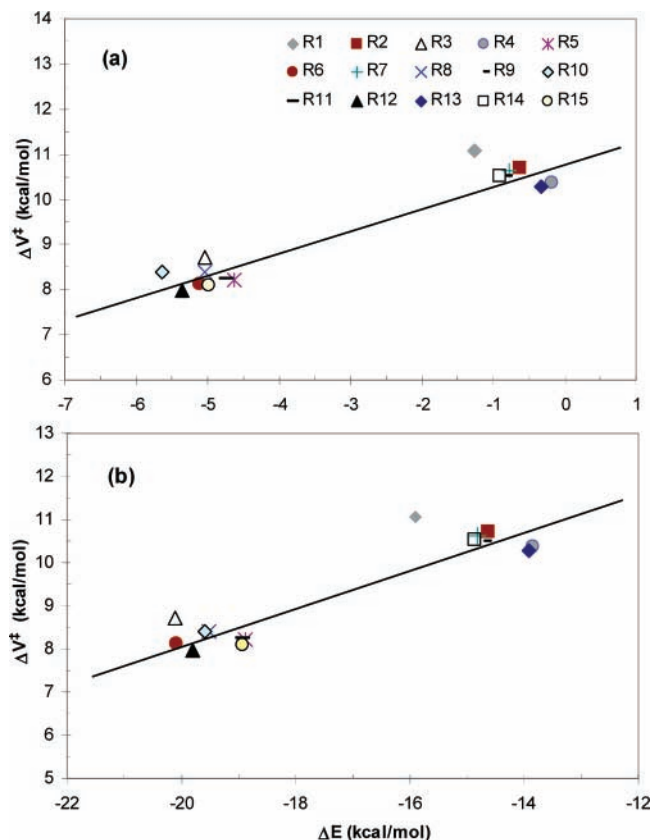


Figure 2. Linear energy relationship plots of the barrier heights, ΔV^\ddagger , calculated at the BH&HLYP/cc-pVTZ level of theory versus the reaction energies, ΔE , computed at (a) BH&HLYP/cc-pVTZ and (b) AM1 levels of theory.

that the LER relationship is excellent at BH&HLYP level but is not as good at the AM1 level of theory. However, if one is interested in rate constants for such reactions, the AM1 should be excluded.

On the basis of the BHG results, we assigned the values of 10.50 and 8.27 kcal/mol to the energy barriers of the terminal and nonterminal carbon sites of the double bond, respectively. It is interesting to note that the averaged deviations of reaction barrier heights estimated from the BHG (0.15 kcal/mol) is smaller than that of the LER, and the maximum deviation (0.46 kcal/mol) is higher. Therefore, this approach can be used to estimate the relative barrier height quickly with an acceptable confidence. The key advantage of this approach is that it does not require any additional information to estimate rate constants.

In conclusion, the barrier height of any reaction in the OH + alkene reaction class can be obtained by using either the LER or BHG approach. The estimated barrier height is then used to calculate the potential energy factor using eq 6. The performance of both approaches is discussed in the error analyses below.

3.2.2. Symmetry Number Factor. The symmetry number factors f_σ were calculated simply from the ratio of reaction symmetry numbers of the arbitrary and reference reactions using eq 3 and are listed in Table 2. The symmetry number of a reaction is given by the number of symmetrically equivalent reaction paths and it can be calculated from the rotational symmetry numbers of the reactant and the transition state.⁴⁰

3.2.3. Tunneling Factor. The tunneling factor f_k is the ratio of the transmission coefficient of reaction R_a to that of reaction R_r. Due to the cancellation of errors in evaluating the tunneling factors, we have shown that the factor f_k can be reasonably estimated using the one-dimension Eckart method.⁴¹ In the

Eckart formulation, the imaginary frequency and the barrier height are used to calculate the tunneling probability for a reaction. Because the barrier heights are grouped into two classes, namely terminal and nonterminal sites of the double-bond carbon (see Potential Energy Factor section), and the imaginary frequencies for reactions at the same class are very similar (see Table S1 in the Supporting Information), the values of the tunneling coefficients for reactions in the same class are expected to be similar. Therefore, the average value for the tunneling factors can be used for the whole group. Simple expressions for the two tunneling factors for terminal and nonterminal carbon sites of the double bond are obtained by fitting to the average calculated values and are

$$f_k = 0.999 - 83.42 \exp[-0.51T^{0.42}] \quad \text{for terminal carbon sites} \quad (9a)$$

$$f_k = 0.978 - 7.55 \exp[-0.0567T^{0.66}] \quad \text{for nonterminal carbon sites} \quad (9b)$$

The correlation coefficients for these fits are larger than 0.999. The two equations are plotted in Figure 3. Table 2 also lists the error analysis of tunneling factors at 300 K. The same tunneling factor expression can be reasonably assigned to different reactions in the same class with the largest unsigned deviation of 0.08 for R₁₃ and the largest percentage deviation of 17.2%. The mean unsigned deviation is 7%, compared to the direct Eckart calculation using reaction information from BH&HLYP/cc-pVTZ level of theory. At higher temperatures, tunneling contributions to the rate constants decrease and thus, as expected, the differences between the approximated values and the explicitly calculated ones also decrease; for example, the maximum error for all reactions is less than 2% at 500 K.

3.2.4. Partition Function Factor. The partition factor includes translational, rotational, internally rotational, vibrational, and electronic components. As pointed out in our previous study,¹¹ the partition function factor f_Q mainly originates from the differences in the coupling between the substituents and the reactive moiety. Its temperature dependence arises from the vibrational and internally rotational components only.

The harmonic partition function factors for reactions R₂–R₁₅ are plotted in Figure 4. The variations in these factors are small, e.g., from 0.5 to 1, and thus it is reasonable to assume that the averaged value from the training set can be applied to the whole class. The averaged values are fitted into the following analytical expression:

$$f_Q = 0.71 - 2.08 \exp[-0.18T^{0.45}] \quad (10)$$

The coupling between substituents with the reactive moiety is believed to account for the partition function factors having values of around 0.7. The total coupling effect is contributed from those of the translational, rotational and vibrational partition function factors. Each reaction class has a specific coupling effect mainly due to the specific/unique reactive moiety. If there is no coupling effect, the values of the partition function factors would be expected to be very close to unity.

For this reaction class, the rotation of the alkyl group (CH₃) along the C–C bond at some reactants, transition states and products as well as the rotation of the hydroxyl (OH) group along the C–O axis at all transition states need to be treated as hindered rotations. We used the approach proposed by Ayala et al.³¹ and the effect of the hindered rotation treatment on the total rate constants represented by the hindered rotation factor can be seen in Figure 5. Particularly, the contribution of such

TABLE 1: Classical Reaction Energies, Barrier Heights, and Unsigned Deviations between Calculated Barrier Heights from DFT and Semiempirical Calculations and Those from LER Expressions and BHG Approach (Zero-Point Energy Correction Not Included; Energies in kcal/mol)

rxn	ΔE		ΔV^\ddagger				$ \Delta V^\ddagger - \Delta V_{\text{estimated}}^\ddagger ^f$		
	DFT ^a	AM1 ^b	DFT ^a	DFT ^c	AM1 ^d	BHG ^e	DFT ^c	AM1 ^d	BHG ^e
R ₁	-1.27	-15.90	11.07	10.15	9.83	10.50	0.92	1.23	0.57
R ₂	-0.63	-14.63	10.71	10.47	10.37	10.50	0.24	0.33	0.20
R ₃	-5.05	-20.12	8.73	8.30	8.05	8.27	0.42	0.68	0.46
R ₄	-0.17	-13.85	10.38	10.69	10.70	10.50	0.31	0.33	0.12
R ₅	-4.63	-18.87	8.21	8.51	8.57	8.27	0.29	0.36	0.06
R ₆	-5.11	-20.08	8.13	8.27	8.06	8.27	0.14	0.07	0.14
R ₇	-0.78	-14.82	10.62	10.39	10.29	10.50	0.23	0.33	0.12
R ₈	-5.04	-19.52	8.40	8.31	8.30	8.27	0.09	0.10	0.12
R ₉	-0.83	-14.69	10.51	10.37	10.35	10.50	0.14	0.16	0.01
R ₁₀	-5.63	-19.58	8.40	8.02	8.27	8.27	0.38	0.13	0.13
R ₁₁	-4.75	-18.93	8.24	8.45	8.55	8.27	0.21	0.31	0.03
R ₁₂	-5.36	-19.80	7.97	8.15	8.18	8.27	0.18	0.21	0.30
R ₁₃	-0.32	-13.92	10.28	10.61	10.67	10.50	0.34	0.39	0.23
R ₁₄	-0.91	-14.87	10.52	10.33	10.27	10.50	0.19	0.25	0.02
R ₁₅	-4.97	-18.92	8.09	8.34	8.55	8.27	0.25	0.46	0.18
MUD ^g							0.24	0.29	0.15

^a Calculated at the BH&HLYP/cc-pVTZ level of theory. ^b Calculated at the AM1 level of theory. ^c Calculated from the LER using reaction energies computed at BH&HLYP/cc-pVTZ level of theory: eq 8a. ^d Calculated from the LER using reaction energies obtained at AM1 level of theory: eq 8b. ^e Estimated from barrier height grouping. ^f ΔV^\ddagger from BH&HLYP/cc-pVTZ calculations; $\Delta V_{\text{estimated}}^\ddagger$ from the linear energy relationship using BH&HLYP/cc-pVTZ and AM1 reaction energies or from barrier height grouping. ^g Mean unsigned deviations (MUD) for reactions R₂–R₁₅.

TABLE 2: Calculated Symmetry Number Factors and Tunneling Factors at 300 K

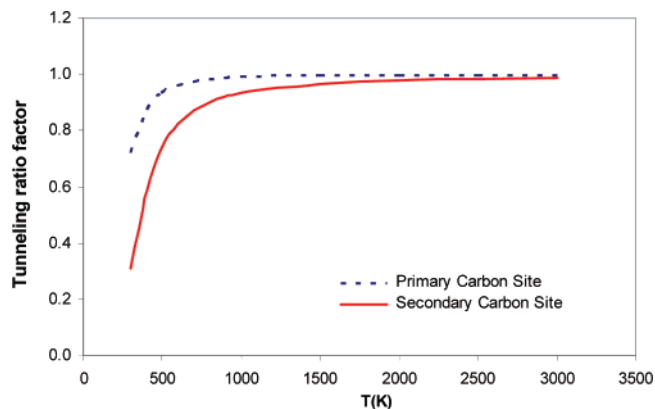
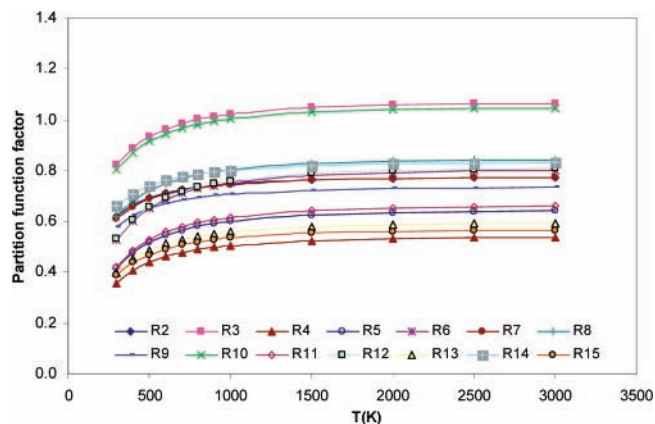
rxn	symmetry no. factor	tunneling ratio factor, f_k			
		Eckart ^a	fitting ^b	deviation ^c	% deviation ^d
R ₁	1.00	80.42 ^f			
R ₂	0.50	0.79	0.72	0.07	8.58
R ₃	0.25	0.37	0.31	0.06	17.18
R ₄	0.50	0.66	0.72	0.06	8.97
R ₅	0.50	0.30	0.31	0.00	1.61
R ₆	0.50	0.29	0.31	0.02	7.50
R ₇	0.50	0.77	0.72	0.05	5.90
R ₈	0.25	0.32	0.31	0.01	3.33
R ₉	0.50	0.74	0.72	0.01	1.99
R ₁₀	0.25	0.33	0.31	0.02	5.53
R ₁₁	0.25	0.30	0.31	0.01	2.07
R ₁₂	0.25	0.27	0.31	0.04	16.53
R ₁₃	0.50	0.64	0.72	0.08	12.80
R ₁₄	0.50	0.74	0.72	0.01	1.86
R ₁₅	0.25	0.29	0.31	0.02	5.54
MUD ^e				0.03	7.10

^a Calculated directly using the Eckart method with the BH&HLYP/cc-pVTZ reaction barrier heights and energies. ^b Calculated by using fitting expression (see eqs 9a and 9b). ^c Unsigned deviation between the fitting and directly calculated values. ^d Percentage deviation (%). ^e Mean unsigned deviations (MUD) and deviation percentage between the fitting and directly calculated values. ^f Tunneling coefficient calculated for reaction (R₁) using the Eckart method with the energetic and frequency information at BH&HLYP/cc-pVTZ.

treatment increases with the temperature increase. In other words, the hindered rotation treatment lowers the total rate constants with the temperature increase. Note that the principal reaction R₁ does not have the internal rotation of the CH₃ group. The averaged values, as applied to the whole class, are fitted into an analytical expression as

$$f_{\text{HR}} = 1.01 - 0.72 \exp[-1332T^{-0.99}] \quad (11)$$

3.2.5. Prediction of Rate Constants. So far we have established the necessary parameters (namely, the potential energy, the symmetry number, the tunneling and the partition function factors) for application of the RC-TST theory to predict rate constants for reactions in the OH + alkene class. The procedure for calculating the rate constants of an arbitrary reaction in this

**Figure 3.** Plots of the tunneling ratio factors f_k as functions of temperature for abstractions of hydrogen from terminal (dotted line) and nonterminal (solid line) carbon sites of the double bond.**Figure 4.** Plots of the harmonic partition function factors for reactions R₂–R₁₅.

class follows: (i) Calculate the potential energy factor using eq 6 with the ΔV_r^\ddagger value of 11.07 kcal/mol. The reaction barrier height can be obtained using the LER approach by employing eq 8a for BH&HLYP/cc-pVTZ reaction energies or eq 8b for AM1 reaction energies or by the BHG approach. (ii)

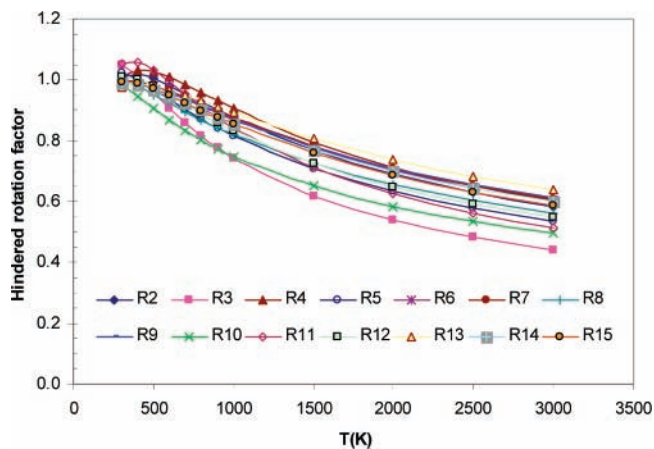


Figure 5. Effect of the hindered rotation treatment on the total rate constants for all reactions R₂–R₁₅ in the temperature range 300–3000 K.

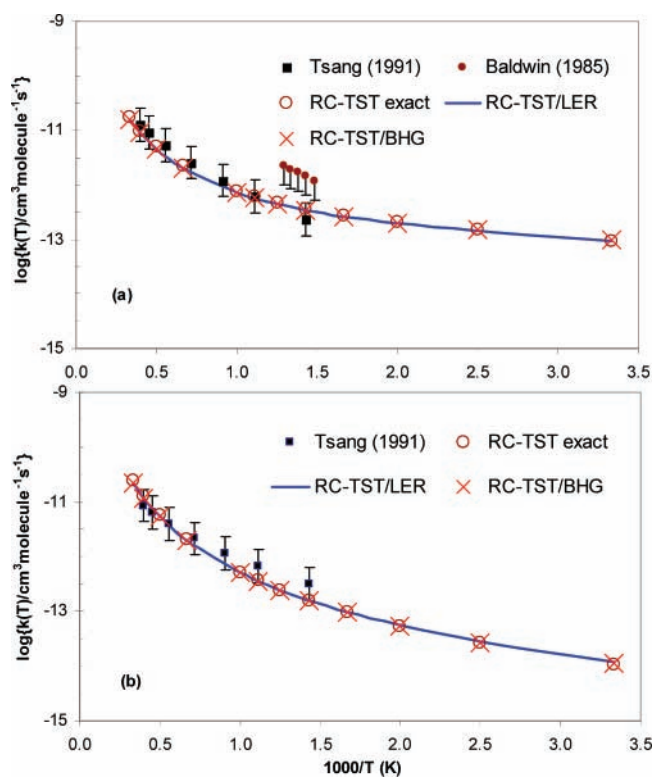


Figure 6. Arrhenius plots of the calculated rate constants using the RC-TST methods for two representative hydrogen abstraction reactions along with the available literature values: (a) OH + C₃H₆ at the terminal carbon; (b) OH + C₃H₆ at the nonterminal carbon. Only the use of the BH&HLYP/cc-pVTZ reaction energies for the LER approach is presented.

Calculate the symmetry number factor from eq 3 or see Table 2. (iii) Compute the tunneling factor using eqs 9a and 9b for terminal and nonterminal carbon sites, respectively. (iv) Evaluate the partition function factor using eq 10 with the hindered rotation treatment correction using eq 11. (v) The rate constants of the arbitrary reaction can be calculated by taking the product of the reference reaction rate constants given by eq 7 with the reaction class factors. Table 3 summarizes the RC-TST parameters for this reaction class.

As mentioned above, the barrier heights can be roughly approximated by the BHG approach (see section 3.2.1). If the BHG barrier heights and the average values for the factors are used, the rate constants are denoted by RC-TST/BHG. The RC-

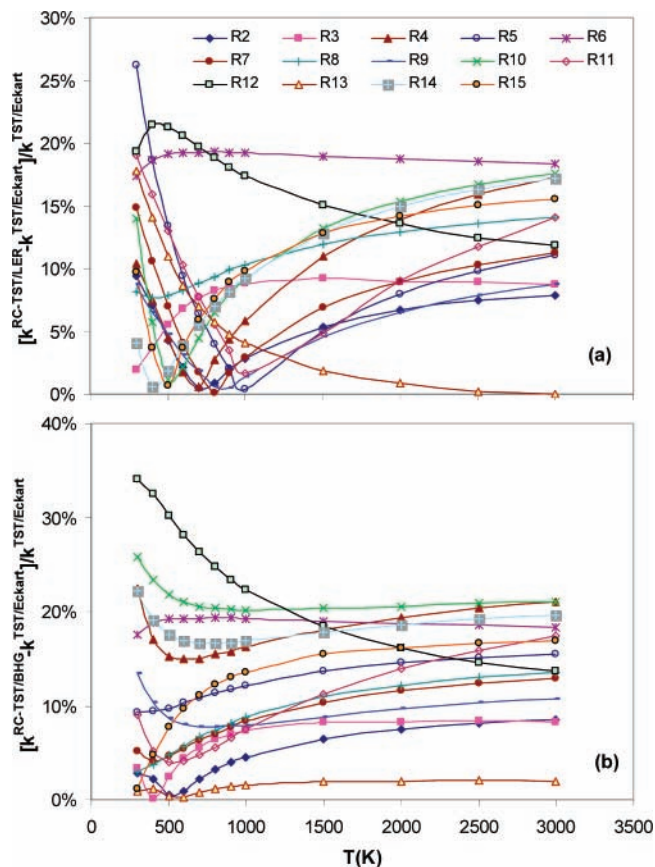


Figure 7. Deviations as functions of the temperature between rate constants calculated with the RC-TST and full TST/Eckart methods for reactions R₂–R₁₅: (a) LER approach, BH&HLYP reaction energies used; (b) BHG approach.

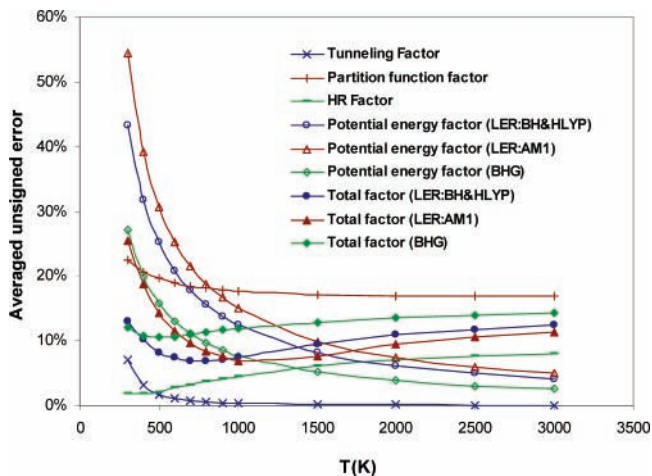


Figure 8. Averaged unsigned errors of the total relative rate factors $f(T)$ (eq 2) and its components, namely the tunneling (f_k), partition function (f_ρ), potential energy (f_v), and hindered rotation correction (f_{HR}) factors, as functions of temperature.

TST/BHG rate constants for any reaction belonging to this reaction class are

$$k(T) = 7.51 \times 10^{-24} T^{3.59} \exp\left[\frac{185}{T}\right] \quad \text{for terminal carbon sites} \quad (12a)$$

$$k(T) = 1.00 \times 10^{-22} T^{3.19} \exp\left[\frac{763}{T}\right] \quad \text{for nonterminal carbon sites} \quad (12b)$$

TABLE 3: Parameters and Formulations of the RC-TST Method for the OH + Alkene → H₂O + Alkenyl Reaction Class (OH + C₂H₄ is the Reference Reaction)

$k(T) = f_{\sigma} f_{\kappa}(T) f_Q(T) f_{HR}(T) f_r(T) k_r(T)$; $f_r(T) = \exp[-((\Delta V^{\ddagger} - \Delta V_r^{\ddagger}))/k_B T]$ T is in Kelvin; ΔV^{\ddagger} and ΔE are in kcal/mol; zero-point energy correction is not included		
f_{σ}	calculated explicitly from the symmetry of reactions (see Table 2)	
$f_{\kappa}(T)$	$f_{\kappa} = 0.999 - 83.42 \exp[-0.51T^{0.42}]$ $f_{\kappa} = 0.978 - 7.55 \exp[-0.056T^{0.66}]$	for terminal carbon sites for nonterminal carbon sites
$f_Q(T)$	$f_Q = 0.71 - 2.08 \exp[-0.18T^{0.45}]$	
$f_{HR}(T)$	$f_{HR} = 1.01 - 0.72 \exp[-1332T^{-0.99}]$	
ΔV^{\ddagger}	LER	$\Delta V^{\ddagger} = 0.4892\Delta E^{BH\&HLYP} + 10.772$ $\Delta V^{\ddagger} = 0.4238\Delta E^{AM1} + 16.572$ $\Delta V_r^{\ddagger} = 11.07 \text{ kcal/mol}^a$
$k_r(T)$ (eq 7)	$k_r(T) = 2.18 \times 10^{-25} T^{4.20} \exp[433/T]$	$[\text{cm}^3 \text{ molecule}^{-1} \text{ s}^{-1}]$
BHG approach	$k(T) = 7.51 \times 10^{-24} T^{3.59} \exp[185/T]$ $k(T) = 1.00 \times 10^{-22} T^{3.19} \exp[763/T]$	for terminal carbon sites for nonterminal carbon sites

^a Calculated value for reaction R1 at the BH&HLYP/cc-pVTZ level of theory.

Because the terminal carbon sites have two hydrogen atoms that can be reasonably considered equivalent in some cases, and the nonterminal sites only have one hydrogen atom, the symmetry factors of 2 and 1 are also included in the rate constant expressions.

To illustrate the theory we selected two reactions R₂ and R₃ whose rate constants are available in the literature. Figure 6a,b show the predicted rate constants of reaction R₂ and reaction R₃ using the RC-TST method and suggested data.^{3,4} In the figure, the “RC-TST exact” notation means that the reaction class factors were calculated explicitly within the TST/Eckart framework rather than using the approximate expressions listed in Table 3. Because the barrier heights obtained from either BH&HLYP/cc-pVTZ or AM1 energies are similar, we can expect their rate constants to be similar.

The rate constants estimated from the RC-TST/LER and RC-TST/BHG approaches are comparable for reactions R₂ and R₃ due to the similar predicted values of the barrier heights, e.g., 10.47 and 10.50 kcal/mol for R₂ from LER and BHG, respectively (see Table 1). The difference in rate constants might be larger for other reactions. Compared to the “RC-TST exact” values, the excellent performance of the RC-TST for these two reactions can be seen in Figure 6. In other words, the derived correlation expressions (see Table 3) can be used to get accurate rate constants for these two reactions.

For reaction R₂ (see Figure 6a), the RC-TST rate constants are within the range of the data suggested by Tsang et al.,³ but they are lower than those estimated by Baldwin et al.⁴ Using the transition state theory (TST) and Tully’s rate data for the OH + C₂H₄ hydrogen abstraction reaction, Tsang et al. suggested rate constants for this reaction in the temperature range 700–2500 K. Baldwin’s data were derived from fitting experimental data for the oxidation of propene to a complex kinetic model; thus such data are less reliable due to the incompleteness and kinetic incorrectness of the model and the procedure to derive the rate constants. For the hydrogen abstraction at the nonterminal carbon of the double bond in propene (reaction R₃), there are only data suggested from Tsang et al. Figure 6b shows the excellent agreement between the RC-TST data and literature data. This comparison only gives a qualitative picture about the performance of this approach because there is a large uncertainty in the reported rate constants for these two reactions.

The accuracy of the RC-TST rate constants depends on several factors. At the fundamental level, it depends on the validity of the transition state theory approximations on which

the RC-TST method is based and the semiclassical SCT tunneling approximations used for the reference (or principal) reaction. It also depends on the accuracy of all approximations that were introduced so that explicit calculations of the transition state structure and frequency are not required. The related errors will be referred to as systematic errors and are discussed below. A better analysis of the efficiency of the RC-TST method would be to compare the RC-TST results with explicit theoretical calculations. As mentioned in our previous studies,^{6,11,15} the RC-TST methodology can be thought of as a procedure for extrapolating rate constants for any given reaction in a class from the reference reaction. Comparisons between the calculated rate constants for a small number of reactions using both the RC-TST and the full TST/Eckart methods would provide additional information on the accuracy of the RC-TST method. To be consistent, the TST/Eckart rate constants of the reference reaction were used in calculation of RC-TST rate constants for this particular analysis rather than using the expression in eq 7. The results for representative reactions R₂–R₁₅ (i.e., the comparisons between the RC-TST/LER and full TST/Eckart methods) are shown in Figure 7, where the relative deviation defined as $(|k^{\text{RC-TST}} - k^{\text{TST/Eckart}}|/k^{\text{TST/Eckart}})$ is plotted versus the temperature. The relative errors are less than 40% for all test cases in both LER and BHG approaches; thus it can be concluded that the RC-TST can predict thermal rate constants for reactions in this class within a factor of 2 when compared to those calculated explicitly using the TST/Eckart method. Note that this analysis for LER is presented for BH&HLYP energies only. One would expect a similar or a slightly worse performance for the case of AM1 energies.

Finally, we examined the systematic errors in different factors in the RC-TST/LER and RC-TST/BHG methods. The total error is affected by the errors in the approximations in the potential energy factor, tunneling factor, partition function factor and the hindered rotation correction factor introduced in the method. The symmetry number factor, however, is “exact”. The deviations/errors between the approximated and exact factors within the TST framework are calculated at each temperature for the reactions in the training set and then averaged over the whole class. For the LER approach, the error in the potential energy factor comes from the use of the LER expression as in eqs 8a and 8b; that of the tunneling factor, from using two eqs 9a and 9b; that of the partition function factor, from using eq 10; and that of hindered rotation corrections, from using eq 11. The results of the analysis of the unsigned errors from different relative rate factors, namely f_{σ} , f_{κ} , f_Q , and f_{HR} used in the RC-

TST method are shown in Figure 8. The results with the RC-TST/BHG (denoted as BHG) are also included in this figure. The error for the potential energy factor arises from using the average barrier heights for terminal and nonterminal carbon sites (BHG approximation). The total error is from the use of the expressions (12a) and (12b) for the terminal and nonterminal carbon sites, respectively. In this figure, we plotted the unsigned errors averaged over all 14 reactions, R₂–R₁₅ as functions of temperature.

The errors of the potential energy factors, f_V , is significantly dependent on the temperature. This can be explained by examining eq 6, which is in the form of the exponential decay of the inverse of the temperature. At low temperature, the potential energy errors are the largest, e.g., 55% at 300 K for the LER approach with the AM1 energies (denoted as LER:AM1), and at high temperature, they are the second smallest ones, e.g., ~5% at 3000 K for the same approach, LER:AM1. In the LER approach, BH&HLYP and AM1 give similar errors for f_V , which are higher than that from the BHG approach. The error of f_V introduced by the BHG approach usually is 50% of that by the LER:AM1. The error of the hindered rotation correction factor increases with the temperature, but other individual errors tend to decrease as the temperature increases. This causes minima of the total errors in the temperature range 300–3000 K, e.g., 700, 1000, and 400 K for the LER: BH&HLYP, LER:AM1, and BHG approaches, respectively.

The total systematic errors due to the use of simple analytical expressions for different reaction class factors are less than 25% in the temperature range 300–3000 K. Even though the BHG has the smallest partition function error, it is not the best approach overall. At 300 K the performance of the BHG gives the smallest error. This can be explained by the error cancellation of other approaches. In fact, the LER:BH&HLYP gives the best performance at the temperature range of interest with the error of less than 15% for the whole temperature range. Even though the LER:AM1 gives the lowest error at temperatures higher than 1000 K, it causes large errors at temperatures below 1000 K, e.g., 25% at 300 K. This error refers simply to the quality of the fitting process and in no sense reflects absolute errors.

In conclusion, the RC-TST/LER approach overall gives a better performance than the BHG; however, the LER needs reaction energy at BH&HLYP/cc-pVTZ and AM1 and the BHG does not need any additional information.

4. Conclusion

We have extended our application of the reaction class transition state theory (RC-TST) combined with the linear energy relationship (LER) and the barrier height grouping (BHG) approaches to the prediction of thermal rate constants for hydrogen abstraction reactions for the OH + alkene class. Combined with the rate constant expression for the reference reaction, OH + C₂H₄, proposed by Liu et al.,³⁷ the RC-TST/LER, where only reaction energy is needed, and RC-TST/BHG, where no other information is required, are both found to be promising methods for predicting rate constants for a large number of reactions in a given reaction class. Our analysis indicates that when compared to explicit theoretical calculations, the averaged systematic errors in the calculated rate constants using either RC-TST/LER or RC-TST/BHG methods are less than 25% over the temperature range 300–3000 K. In addition, we found that the estimated rate constants using either approach are in good agreement with available data in the literature.

Acknowledgment. This research is funded by the U.S. Air Force Scientific Office for Research (Grant No. FA9550-06-1-0376).

Supporting Information Available: A table of optimized geometries and calculated frequencies of all species and transition states at the BH&HLYP/cc-pVTZ level of theory. This material is available free of charge via the Internet at <http://pubs.acs.org>

References and Notes

- (1) Warnatz, J. In *Combustion Chemistry*; Gardiner, W. C., Jr., Ed.; Springer-Verlag: New York, 1984.
- (2) NIST Chemical Kinetics Database, Version 7.0 (Web Version), Release 1.4, <http://kinetics.nist.gov/kinetics/index.jsp>.
- (3) Tsang, W. *J. Phys. Chem. Ref. Data* **1991**, *20*, 221.
- (4) Baldwin, R. R.; Hisham, M. W. M.; Walker, R. W. *Symp. Int. Combust. Proc.* **1985**, *20*.
- (5) Tully, F. P. *Chem. Phys. Lett.* **1988**, *143*, 510.
- (6) Truong, T. N. *J. Chem. Phys.* **2000**, *113*, 4957.
- (7) Sumathi, R.; Carstensen, H. H.; Green, W. H., Jr. *J. Phys. Chem. A* **2001**, *105*, 6910.
- (8) Huynh, L. K.; Ratkiewicz, A.; Truong, T. N. *J. Phys. Chem. A* **2006**, *110*, 473.
- (9) Huynh, L. K.; Truong, T. N. *Theor. Chem. Acc.*, in press.
- (10) Huynh, L. K.; Zhang, S.; Truong, T. N. *Combust. Flame*, in press.
- (11) Zhang, S.; Truong, T. N. *J. Phys. Chem. A* **2003**, *107*, 1138.
- (12) Violi, A.; Truong, T. N.; Sarofim, A. F. *J. Phys. Chem. A* **2004**, *108*, 4846.
- (13) Kungwan, N.; Truong, T. N. *J. Phys. Chem. A* **2005**, *109*, 7742.
- (14) Truong, T. N.; Duncan, W. T.; Tirtowidjojo, M. *Phys. Chem. Chem. Phys.* **1999**, *1*, 1061.
- (15) Truong, T. N.; Maity, D. K.; Truong, T.-T. *J. Chem. Phys.* **2000**, *112*, 24.
- (16) Evans, M. G.; Polanyi, M. *Proc. R. Soc.* **1936**, *154*, 133.
- (17) Evans, M. G.; Polanyi, M. *Trans. Faraday Soc.* **1936**, *32*, 1333.
- (18) Polanyi, J. C. *Acc. Chem. Res.* **1972**, *5*, 161.
- (19) Frisch, M. J.; Trucks, G. W.; Schlegel, H. B.; Scuseria, G. E.; Robb, M. A.; Cheeseman, J. R.; Montgomery, J. A., Jr.; Kudin, K. N.; Burant, J. C.; Millam, J. M.; Iyengar, S. S.; Tomasi, J.; Barone, V.; Mennucci, B.; Cossi, M.; Scalmani, G.; Rega, N.; Petersson, G. A.; Nakatsuji, H.; Hada, M.; Ehara, M.; Toyota, K.; Fukuda, R.; Hasegawa, J.; Ishida, M.; Nakajima, T.; Honda, Y.; Kitao, O.; Nakai, H.; Klene, M.; Li, X.; Knox, J. E.; Hratchian, H. P.; Cross, J. B.; Adamo, C.; Jaramillo, J.; Gomperts, R.; Stratmann, R. E.; Yazyev, O.; Austin, A. J.; Cammi, R.; Pomelli, C.; Ochterski, J. W.; Ayala, P. Y.; Morokuma, K.; Voth, G. A.; Salvador, P.; Dannenberg, J. J.; Zakrzewski, V. G.; Dapprich, S.; Daniels, A. D.; Strain, M. C.; Farkas, O.; Malick, D. K.; Rabuck, A. D.; Raghavachari, K.; Foresman, J. B.; Ortiz, J. V.; Cui, Q.; Baboul, A. G.; Clifford, S.; Cioslowski, J.; Stefanov, B. B.; Liu, G.; Liashenko, A.; Piskorz, P.; Komaromi, I.; Martin, R. L.; Fox, D. J.; Keith, T.; Al-Laham, M. A.; Peng, C. Y.; Nanayakkara, A.; Challacombe, M.; Gill, P. M. W.; Johnson, B.; Chen, W.; Wong, M. W.; Gonzalez, C.; Pople, J. A. *Gaussian 03*, revision A.1; Gaussian, Inc.: Pittsburgh, PA, 2003.
- (20) Becke, A. D. *J. Chem. Phys.* **1993**, *98*, 1372.
- (21) Lee, C.; Yang, W.; Parr, R. G. *Phys. Rev.* **1988**, *37*, 785.
- (22) Truong, T. N. *J. Chem. Phys.* **1994**, *100*, 8014.
- (23) Truong, T. N.; Duncan, W. *J. Chem. Phys.* **1994**, *101*, 7408.
- (24) Lynch, B. J.; Fast, P. L.; Harris, M.; Truhlar, D. G. *J. Phys. Chem. A* **2000**, *104*, 4811.
- (25) Zhang, Q.; Bell, R.; Truong, T. N. *J. Phys. Chem. A* **1995**, *99*, 592.
- (26) Wang, D.; Violi, A. *J. Org. Chem.* **2006**, *71*, 8365.
- (27) Chae, K.; Violi, A. *J. Org. Chem.* **2007**, *72*, 3179.
- (28) Dunning, T. H. Jr. *J. Chem. Phys.* **1989**, *94*, 5523.
- (29) Dewar, M.; Thiel, W. *J. Am. Chem. Soc.* **1977**, *99*, 2338.
- (30) Truong, T. N.; Nayak, M.; Huynh, H. H.; Cook, T.; Mahajan, P.; Tran, L.-T. T.; Bharath, J.; Jain, S.; Pham, H. B.; Boonyasiriwat, C.; Nguyen, N.; Andersen, E.; Kim, Y.; Choe, S.; Choi, J.; Cheatham T. E., III; Facelli, J. C. *J. Chem. Inf. Model.* **2006**, *46*, 971.
- (31) Ayala, P. Y.; Schlegel, H. B. *J. Chem. Phys.* **1998**, *108*, 2314.
- (32) Pitzer, K. S.; Gwinn, W. D. *J. Chem. Phys.* **1942**, *10*, 428.
- (33) Li, J. C. M.; Pitzer, K. S. *J. Phys. Chem.* **1956**, *60*, 466.
- (34) Baulch, D. L. C. C. J.; Cox, R. A.; Esser, C.; Frank, P.; Just, Th.; Kerr, J. A.; Pilling, M. J.; Troe, J.; Walker, R. W.; Warnatz, J. *J. Phys. Chem. Ref. Data* **1992**, *21*, 411.

- (35) Westbrook, C. K. T., M. M.; Pitz, W. J.; Malte, P. C. *Symp. Int. Combust. Proc.* **1988**, 22, 863.
- (36) Liu, A.; Mulac, W. A.; Jonah, C. D. *J. Phys. Chem.* **1988**, 92, 3828.
- (37) Liu, G.; Ding, Y.; Li, Z.; Fu, Q.; Huang, X.; Sun, C.; Tang, A. *Phys. Chem. Chem. Phys.* **2002**, 4, 1021.
- (38) Senosiain, J. P.; Klippenstein, S. J.; Miller, J. A. *J. Phys. Chem. A* **2006**, 110, 6960.

- (39) Huynh, L. K.; Panasewicz, S.; Ratkiewicz, A.; Truong, T. N. *J. Phys. Chem. A* **2007**, 111, 2156.
- (40) Duncan, W. T.; Bell, R. L.; Truong, T. N. *J. Comput. Chem.* **1998**, 19, 1039.
- (41) Miller, W. H. *J. Am. Chem. Soc.* **1979**, 101, 6810.
- (42) Violi, A.; Sarofim, A. F.; Truong, T. N. *Combust. Flame* **2001**, 126, 1506.